



ELSEVIER

Contents lists available at [SciVerse ScienceDirect](http://www.sciencedirect.com)

Fire Safety Journal

journal homepage: www.elsevier.com/locate/firesaf

Numerical simulation of the interaction between two fire fronts in grassland and shrubland

Dominique Morvan^{a,*}, Chad Hoffman^b, Francisco Rego^c, William Mell^d

^a Aix-Marseille Univ, Laboratoire M2P2 UMR CNRS 6181, UNIMECA Technopôle de Château Gombert, 60 rue Joliot Curie, 13453 Marseille Cedex 13, France

^b Department of Forest and Range Stewardship, Colorado State University, Fort Collins, CO, USA

^c ISA-CEABN Tapada da Ajuda 1349-017, Lisbon, Portugal

^d US Forest Service, Pacific Wildland Fire Sciences Lab, 400 N. 34th Street, Suite 201, Seattle, WA 98103, USA

ARTICLE INFO

Article history:

Received 24 March 2010

Received in revised form

21 July 2011

Accepted 25 July 2011

Keywords:

Fire behaviour

FIRESTAR

WFDS

Back firing

ABSTRACT

The objective of this paper was to evaluate the potential for fully physical fire models to simulate the interactions between two converging fire fronts (a head fire and a back fire), in conditions similar to those encountered during suppression fire operations. The simulations were carried out using two fully physical models: FIRESTAR, in two dimensions, and Wildland Fire Dynamics Simulator, in three dimensions. Each modelling approach numerically solves a set of balance equations (mass, momentum, energy, etc.) governing the behaviour of the coupled system formed by the vegetation and the surrounding atmosphere. Two fuel profiles were tested: homogeneous grassland similar to landscapes in Australia and a shrubland representative of Mediterranean landscape (garrigue). Results from the two-dimensional and three-dimensional simulations were used to investigate how the two fire fronts interact together and mutually modify, or not, their own behaviour before merging. The results of these simulations showed that the merging of two fire fronts can result in a quick increase in fire-line intensity or in flame height. We concluded that physics-based simulations do reproduce reasonable and expected head- and back-fire interactions, but more work is needed to further understand the accuracy of such predictions.

© 2011 Elsevier Ltd. All rights reserved.

1. Brief summary

The objective of this paper is to evaluate the potential for physically based fire models to simulate the interactions between a head fire and a back fire, in conditions similar to those encountered during suppression fire operations. In this study, we focussed our efforts to identify how a head fire and a back fire can interact and at what distance this interaction can be detected, how the air flow around the two fire fronts can contribute to this interaction and what were the significant events before and during the merging of the two fire fronts. We concluded that physics-based simulations do reproduce reasonable and expected fire behaviour.

2. Introduction

To stop the propagation of a wildfire or reduce its intensity, fire fighters rely on reducing one side of the fire triangle: fuel,

heat and oxygen. Considering that it is difficult to directly affect the oxygen supplying the fire front, in an unconfined and for a fully developed fire, fire fighters typically focus their efforts on reducing the heat released by the fire, using water or foam, or on eliminating the fuel located between the fire front and a control line. The reduction of fuel can be accomplished using mechanical means (bulldozer) or using a suppression fire (also called a counter fire or a back fire), which is a traditional technique of fire fighting [1]. During the last few decades, this technique has been reintroduced as an alternative tool when classical terrestrial or aerial means were non-operational or not sufficiently efficient. Goldammer and De Ronde [2] formally distinguished two suppression fire techniques: burn-out operations and back-firing operations. Burn-out operations use techniques very similar to prescribed burning, with the goal of burning the vegetation located between the main fire and the control line. The use of back-fire operations is more aggressive, and consists of igniting a fire line (back fire) as close as possible to the main fire front. In this case, it is expected that the main fire front will generate an in-draught flow, facilitating the propagation of the back fire. If successful, the fires fronts propagate towards each other and merge, resulting in the consumption of the fuel between the

* Corresponding author.

E-mail address: dominique.morvan@univmed.fr (D. Morvan).

ignition point of the back fire and the main fire front. The back fire, having burned all the available solid fuel ahead of the main fire front, blocks the progression of the wildfire and causes the main front to rapidly extinguish [1–3]. Very few studies have been published on this subject, and it is not well known at what distance (as a function of the fire-line intensity) a wildfire can interact with a back fire (in-draught distance).

In a review paper dedicated to the interaction between wind and fires, Pitts [4] dedicated a section to the problem of multiple fire interactions. This problem was studied initially to understand how individual fuel sources can merge to form a single cohesive fire front. Depending on burner distribution, this experimental study showed that the fuel consumption rate reached a maximal value, and then decreased because of the limitation on air supply caused by adjacent burners. More recently, Roxburgh and Rein [5] performed two-dimensional (2D) numerical simulations using the Fire Dynamics Simulator (FDS) developed by the Building and Fire Research Laboratory (BFRL-NIST), to study the in-draught flow generated ahead of a wildfire by the convection plume. In this study, the fire was represented as a fixed line burner. A number of cases were considered, using a wide range of fire intensities (from 1 to 10 MW/m) and wind speed velocities (from 1 to 15 m/s). Considering the behaviour of the flow field ahead of the fire front, the authors distinguished three zones: zone 1 nearest the fire front, where the wind field was directly affected by flame dynamics, zone 2 located at the maximum furthest distance from the main fire front, at which a backing fire is influenced by the winds from the main fire front, zone 3 located at a distance from the main fire front, such that the behaviour of the backing fire is dominated by the external atmospheric flow. These numerical results highlighted the extension of zone 2 as a function of the fire intensity. The results also indicated that the maximum distance away from the main fire front, where a back fire can benefit from the in-draught flow, ranged from 15 to 70 m. Experimental infrared analysis of the trajectory of soot particles showed that updraught flow measured in a plume above an intense crown fire can reach 50–60 m/s [6]. By a mass balance mechanism, the air rising in the plume is then replaced by ambient air pulled towards the base of the fire. This is the mechanism that is at the origin of the in-draught flow in the vicinity of a fire front. Using coupled atmosphere–fire–environment models, Coen [7] and Morvan et al. [8,9] showed that two mechanisms can contribute to the interaction between two fire fronts: the plume–atmosphere interaction (at the origin of the in-draught flow) and the shelter effect resulting from the action of the head fire upon the back fire. This problem was also studied experimentally in a laboratory, for surface fires ignited in a fuel bed. The analysis of the air flow at the vicinity of the two surface fires highlighted that before the two fire fronts have merged, the flames have oscillated in phase and the two smoke columns gradually have merged into a single one smoke column [10]. As part of the EU FP6 Program FIREPARADOX [11,12], a set of experimental fires and numerical simulations [13] were conducted with the goal to study the conditions of success of suppression fires. The experiments were conducted in Mediterranean mixed heathland fuels (fuel depth ranged between 40 and 60 cm, fuel load from 1.5 to 2.5 kg/m²), for light to moderate breeze (average wind velocity less than 7.9 m/s). The experiments showed clearly that the air flow was significantly affected by the fire fronts. For a gentle breeze (wind < 5.4 m/s), the back fire kept a rate of spread (ROS) that was almost constant (~0.02 m/s). After a short period of acceleration, following the ignition, the head fire reached a quasi-steady state regime of propagation (ROS~0.33 m/s). When the distance separating the two fire fronts was equal to 20 m, the head fire accelerated suddenly (ROS~0.63 m/s). For light air on the Beaufort wind scale (wind < 1.5 m/s), the back fire and the head fire

propagated with ROS values equal to 0.03 m/s (back fire) and 0.25 m/s (head fire), respectively. Just before the collision, the progression of the two fire fronts was accelerated to 0.45 m/s (back fire) and 0.61 m/s (head fire). For these moderate wind conditions, the in-draught flow, ahead of the main fire, modified the behaviour of the back fire, which became a secondary head fire (i.e. a fire propagating in the same direction as the apparent local wind), and the interaction distance observed between the two fire fronts was equal to 70 m [12]. After this first set of experimental fires, we can conclude that it is not so easy to define the ideal situation to ignite a back fire during a suppression fire operation, as the conditions necessary to generate a stable in-draught flow ahead of the main fire front are not well defined. For example, it was observed in the experiments that some conditions favourable for the entrainment of the back fire towards the head fire (in-draught flow) can also contribute to modifying considerably the ROS of the back fire, increasing its intensity and degrading the safety of fire fighters.

One of the objectives of the FIREPARADOX project was to investigate the usefulness and ability for physics-based simulation methods to capture the general behaviour reported in the field experiments and in the literature. If physics-based simulations perform sufficiently well, they may lead to the development of better guidelines for the use of back fires and provide additional research hypotheses.

3. Physical consideration and mathematical model

The present study was dedicated to the propagation of fires for two fuel complex: a grass-dominated fuel bed and a shrub-dominated fuel bed. To perform these numerical simulations, we used two fully physical models: one using a 2D formulation (FIRESTAR) and the other one using a three-dimensional (3D) formulation (Wildland Fire Dynamics Simulator, WFDS). Both of these approaches adopted a multiphase formulation, based on an approach proposed by Grishin [13] to represent the physical mechanisms governing the behaviour of the coupled system formed by the vegetation and the surrounding atmospheric flow. The heterogeneous structure of the vegetation was taken into account using a set of solid fuel families that represent the fine fuel elements (thickness smaller than 6 mm) contributing directly to the propagation of the fire, namely foliage, branches and twigs.

In FIRESTAR, the number of fuel types coexisting in an elementary control volume was not limited, allowing the representation of complex solid fuel mixing, including more or less fine fuel elements and dead and living fuel. In the WFDS implementation used here, only one fuel element type (representing an average value) was defined in an elementary control volume. Fuel elements submitted to intense heat transfer by convection and radiation coming from the flame were dehydrated and decomposed (pyrolysis process) into gas (mainly CO and CO₂) and solid (charcoal) products within the simulations. The gaseous combustion in the flame was calculated assuming that the reaction rate was mainly limited by the turbulent mixing between the gaseous pyrolysis products and the ambient air (eddy dissipation combustion model). Both radiation and convective heat transfer between the flame (soot–gas mixing) and vegetation were included. The interaction between the atmospheric boundary layer flow and the vegetation layer was also taken into account in the simulations, in adding volume drag force and heat and mass transfer terms in the equations governing the turbulent fluid flow (momentum, turbulent kinetics energy, turbulent dissipation rate, energy and chemical species). See Refs. [14–16] for a detailed description of the FIRESTAR model and Ref. [17] for a detailed description of the WFDS model. The

FIRESTAR model was developed during the European project FIRESTAR and FIREPARADOX (5th and 6th EU Framework Programme), and was intensively tested on various conditions in grassland, Mediterranean shrubland and boreal forest [14–16] and compared with data collected during campaigns of experimental fires [18–20]. The WFDS model has been tested using the results of Australian grassland fires [18,21] and provided good predictions of the fire-line propagation and of the head fire spread dependence on the head fire width.

Compared to a previous numerical study carried out using FIRESTAR for surface fires in grassland [15], the present numerical simulations were performed using an additional physical module to take into account temperature fluctuations in radiation heat transfer. Radiation heat transfer was identified as the main heat transfer mechanism contributing to the propagation of back fires. In considering the non-linear form of terms associated with this physical phenomenon, it is relatively easy to demonstrate [22] that the term from the turbulence/radiation interaction [23] constitutes a significant contribution to the energy balance equation.

4. Numerical simulations: initial and boundary conditions

Two-dimensional simulations were carried out using FIRESTAR, for a homogeneous fuel layer similar to those in experiments performed in grassland in Australia [18,21], and in a more complex heterogeneous fuel configuration, representing a Mediterranean shrubland for several different wind speeds (the fuel properties are summarised in Table 1). A total of 24 simulations were performed with FIRESTAR, 9 in the Australian grassland and 15 in the Mediterranean shrubland fuels. Both fuel types were simulated with a head fire only, a back fire only and both a head and back fire. The Australian grass simulations were conducted with 3 different wind speeds, while the Mediterranean shrublands were simulated for 5 different wind speeds.

The overall domain size of these simulations was 130 by 30 m for the X and Z directions, respectively. To sustain the propagation of the back fire, mainly governed by radiation heat transfer, the mesh size in the streamwise δ_x and vertical direction δ_z was chosen such that $\delta_x = 2\delta_R$ and $\delta_z = \delta_R/2$, where δ_R is the extinction length scale (equal to 0.24 m in Australian grassland and ranges

between 0.25 and 0.31 m in Mediterranean shrubland, chosen for the present simulations). To obtain an accurate representation of turbulent structures induced by the shearing effect above the vegetation layer [24], we verified that δ_z was smaller than that of the turbulence integral length scale (strongly correlated to the fuel depth H_{FUEL}), by imposing the constraint $\delta_z < H_{\text{FUEL}}/4$. To restrain the propagation of the two fire fronts (main fire and back fire), the fuel was distributed between two points along the streamwise direction: $X=10$ and 110 m (see Fig. 1). As shown in Fig. 1, a control line was created behind the back fire between $X=110$ and 130 m. The initial wind velocity profile (initial conditions and boundary conditions are at the left-hand side of the computational domain) was set as a logarithmic function:

$$U_x = U_H \ln\left(\frac{Z+Z_0}{Z_0}\right) \quad (1)$$

The value of U_H was adapted in order to impose a velocity level 2 or 10 m above the ground level (for a nude soil, $Z_0=0.01$ m). After a set of numerical experiments, the initialisation procedure to begin the simulations was defined as the following. To stabilise the initial air flow conditions, the flow was computed during the first 20 s without any source of energy, then, two burners were activated simultaneously to ignite the fuel at the two edge points of the vegetation layer. Even if this procedure did not correspond to real operational conditions, we can estimate that the distance initially separating the two ignition lines was sufficient to consider that the conditions of propagation for the head fire were fully established before the two fire fronts merged. The Australian grassland simulations were performed for 3 values of the 2 m open wind velocity $U_2=1.0, 2.0$ and 4.0 m/s (see Fig. 1), while the Mediterranean shrubland fuels were simulated using 5 values for the 10 m open wind velocities (U_{10}), ranging from 2 to 16 m/s. In addition to the 2D numerical simulations using FIRESTAR, we conducted 3D numerical simulations using WFDS [17] for the Australian grass fuel type. The WFDS simulations were carried out using a large computational domain consisting of $1500 \text{ m} \times 1500 \text{ m} \times 200 \text{ m}$, in the X, Y and Z directions, respectively. The fuel bed was positioned at the centre of the domain, as a $100 \text{ m} \times 100 \text{ m}$ plot. The length of the grassland plot and the location of the head- and back-fire ignition was the same as the FIRESTAR simulations. A 30 m wide strip of grass was located around the border of the Australian grass fuels plot, and was not allowed to burn. The grid configuration was similar to the one used in [17]. The grid size used in the WFDS simulations was uniform and equal to 1.66 m along the horizontal directions (X and Y), while the grid size was vertically stretched from 1.38 m near the ground to 5.5 m at 200 m above the ground. The computational domain surrounding the fine mesh had the same grid resolution in the vertical direction and a 3.33 m resolution in the horizontal directions. The wind flow through the upwind boundary and initially throughout the domain was

$$U_x = U_2 \left(\frac{Z}{2}\right)^{1/7} \quad (2)$$

Table 1
Physical properties characterising the fuel layer used for the calculation performed in grassland [19].

Fuel density (kg/m^3)	514
Fuel packing ratio $\times 10^3$	1.36
Fuel moisture content (%)	6
Fuel depth (m)	0.5
Fuel load (t/ha)	7
Surface area to volume ratio (m^{-1})	12240
Leaf area index (LAI)	4.16

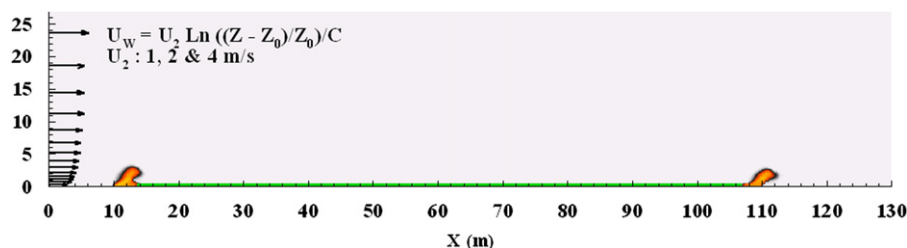


Fig. 1. Interaction between two fire fronts in grassland: geometry and wind velocity profile imposed at the inlet of the computational domain.

(the other velocity components: $U_y=U_z=0$) where U_2 is the open wind velocity at a height of 2 m. The wind speed at 2 m was set at 2 m/s. These two wind velocity profiles (Eqs. (1) and (2)), imposed at the inlet of the computational domains, presented some differences (the two studies were initially developed separately). Nevertheless, in considering that past the vicinity of the inlet of the computational domain, the velocity profile was rapidly affected by the presence of the vegetation, we can consider that this small difference concerning the inlet wind profile did not play a great role in the behaviour of the fires. In FIRESTAR, the boundary conditions at the downstream and at the top boundaries were treated as the following: we assumed that the pressure field was not affected by the fluid flow and that at each time step, the local magnitude and the direction (inflow or outflow) of the flow was evaluated to verify a mass balance equation (some additional iterations were also added to be sure that the momentum equations were also correctly verified at the boundaries). Concerning the scalar transported variables, we have adopted the following dynamical procedure: for outflow boundary conditions, we have imposed that the second normal derivatives were equal to zero, for inflow boundary conditions, we have imposed standard conditions corresponding to the initial state of the atmosphere. At the bottom, we assumed impermeable and adiabatic boundary conditions, the turbulent boundary layer was treated using a standard wall function approach, excepted in regions affected by vertical motions (e.g. near the fire fronts). The procedure adopted for WFDS is much more simple, free boundary conditions (i.e. the values at the boundary were assumed to be

equal to the values calculated at the first points located inside the computational domain) were imposed at the two lateral boundaries, downstream and at the top. Similar to the FIRESTAR calculations, in WFDS, the two fire fronts were ignited after an initialisation time, necessary to initiate the turbulent flow field. A total of two simulations were conducted using WFDS, the first one was a standalone head fire simulation and the second one was a simulation including both a head fire and a back fire. For the head fire only simulation, the head fire was ignited as a 100 m long strip at the beginning of the fuel bed. For the fire-front interaction simulations, the head and back fire were ignited simultaneously as 100 m long fire strips.

5. FIRESTAR results for grass fires

The temperature field and the velocity vectors of the gaseous phase obtained for a wind speed $U_2=2$ m/s ($U_{10}=2.6$ m/s) are shown in Fig. 2. These snap shots show 3 phases of head-fire/back-fire interactions reported both in suppression fire operations and in the simulations conducted by Roxborough and Rein [5]:

- Phase 1: free propagation in opposite directions of the two fire fronts (the head fire on the left and the back fire on the right) converging towards the same meeting point (Fig. 2a).
- Phase 2: the phase during which the two fire fronts can interact, just before their merging (Fig. 2b).
- Phase 3: the merging of the two fire fronts in a single fire (Fig. 2c).

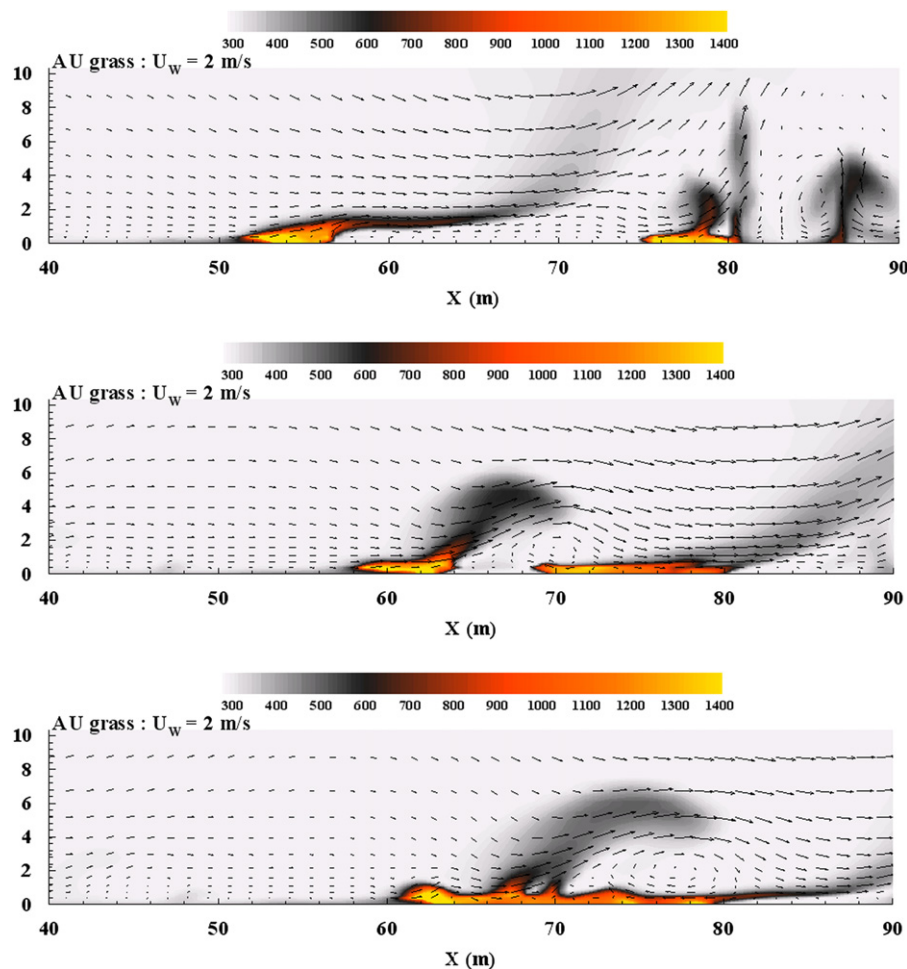


Fig. 2. Temperature and velocity vectors calculated during the propagation of a head fire (left) and a back fire (right) in a grassland 68, 78 and 82 s after the simultaneous ignition of the two fires and for a wind speed $U_2=2$ m/s ($U_{10}=2.6$ m/s).

Table 2
Physical properties characterising the fuel layer used for the calculation performed in shrubland (from experimental values collected on the field).

	Leaves	Twigs (0–2 mm)	Twigs (2–6 mm)	Grass
Fuel density (kg/m ³)	810	900	930	440
Fuel packing ratio (average) × 10 ³	2.175	1.15	2.175	1
Fuel moisture content (%)	30	30	30	5
Fuel depth (m)	0.75	0.75	0.75	0.25
Fuel load (t/ha)	33			
Surface area to volume ratio (m ⁻¹)	5920	2700	1000	20,000
Leaf area index (LAI)			6.00	

In our simulations, the air flow in the vicinity of the two fire fronts was greatly affected by the presence of the opposite fires Table 2. This resulted in a reduction of the influence of the ambient wind flow on the radiation heat transfer between the flame and the unburned vegetation located ahead of the fire front, thereby influencing the propagation of both head fire and back fire. For $U_2=2$ m/s (light breeze), our results indicate that the ROS characterising the head fire (ROS=0.71 m/s) was a little bit larger than the values observed for the back fire (ROS=0.54 m/s). However, the ratio between the two ROS values (~1.3) was not as large as was expected based on observations in the field. Experimental fires carried out in a shrubland [11,12] (fuel moisture conditions (FMCs) for dead and alive fuel ranged between 8% and 80%), for a moderate slope (<11%) and low wind speed conditions (<1.4 m/s), had exhibited that the head fire propagated twice as fast as the back fire. This could be due to the particular propagation regime induced for moderate wind conditions, i.e. it is regularly admitted that a back fire propagates at a speed more or less equal to the value observed for a surface fire without wind. The very low FMCs (FMC=6%) used for this simulation can also explain that the behaviour of the fire was more affected by the FMC than by the relative orientation between the direction of propagation and the wind direction. For fires propagating in weak wind conditions, the air flow in the vicinity of the two fire fronts was greatly affected by the fire itself, reducing in the same way the influence of the wind flow, and the propagation of both the head fire and back fire was mainly governed by the radiation heat transfer between the flame and the unburned vegetation located ahead of the fire front. The sum of the two fire-line intensities (head fire plus back fire) (assuming a heat of combustion equal to 18 MJ/kg) was equal to 5998 kW/m, and was nearly equal to the sum of fire intensities calculated in simulating the head fire and the back fire separately, for which we found a value equal to 5691 kW/m. The time history of temperature (Fig. 3) calculated for two points located 0.5 m above the ground level, at $X=60$ m (P1) and $X=80$ m (P2), on both side of the meeting point of the two fires (~ $X=68$ m), also highlighted the differences in behaviour of the two fire fronts. At the first point (P1), we can see the travelling of the head fire, characterised by a sharp increase of the temperature signal. The maximum temperature calculated at this point was nearly equal to 1440 K, and we evaluated that the fire residence time (τ) of the head fire was equal to 13 s. At the second point (P2) (affected by the travelling of the back fire), the temperature signal was more extended in time, the fire residence time was multiplied by a factor of 3.5 ($\tau=46$ s), and the temperature reached a maximal value sensibly smaller than for the head fire, equal to 840 K.

The ROS (evaluated during the steady state phase) obtained for 3 values of 10 m open wind velocity U_{10} ($U_{10}=1.3U_2$) are shown in Fig. 4, for calculations simulating a suppression fire operation (FIRESTAR head fire and back fire) and compared with results

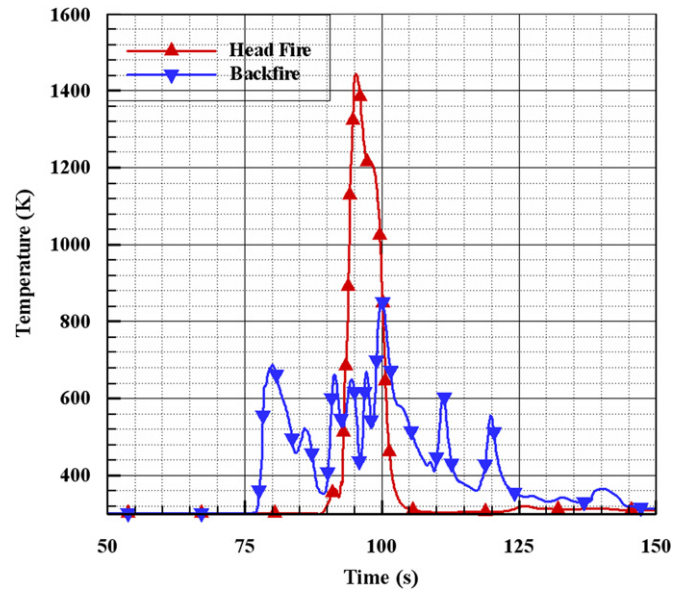


Fig. 3. Temperature–time history for two points located at $X=60$ and 80 m, respectively, affected by the arrival of the head fire and the back fire ($U_2=2$ m/s).

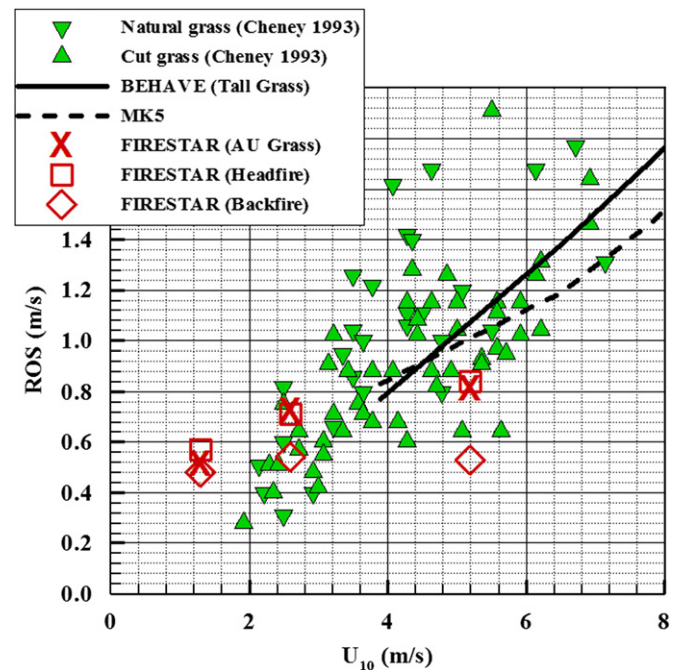


Fig. 4. Rate of spread (ROS) versus 10 m open wind speed (U_{10}) of the head fire and the back fire compared with the values during the propagation of a single surface fire by simulation (FIRESTAR AU Grass) and experimentally [19].

obtained for a single fire propagating along the wind direction (FIRESTAR AU Grass). The results were also compared with experimental data collected during experimental fires in similar conditions [18,21]. We also added the predictions obtained using empirical (MK5) and semi-empirical (BEHAVE) operational models. These results showed that, as indicated previously, for these conditions, except during the short time before the merging of the two fire fronts, the propagation of the head fire was not significantly affected by the presence of the back fire, and the ROS values with and without back fire were the same (see Fig. 4). We also noticed that the ROS associated with the back fire was weakly affected by the wind flow. This result was not surprising

considering that the back fire was isolated from the action of the wind flow by the presence of head fire, and that the propagation of the back fire was mainly piloted by radiation heat transfer between the flame (pushed on the downstream side) and the unburned vegetation.

6. FIRESTAR results for shrub fires

For Mediterranean shrubland fuels, we observed a sustained propagation for both the head fire and back fires, except for $U_{10}=2$ and 16 m/s ($U_{10}=1.3U_2$), for which we noticed a more or less rapid extinction of back fire. Fig. 5 shows temperature fields calculated 40 and 105 s after ignition of the head and back fires (occurring 20 s after the beginning of the calculation), for a wind speed $U_{10}=4$ m/s. Comparing the two temperature fields, we notice that the flame height increases during the merging phase of the head fire and back fire at $t=105+20=125$ s (see also Fig. 6). This sudden increase in flame height has often been reported by fire fighters and foresters during suppression fire operations in fuel beds similar to the ones simulated here. In Fig. 6, the time histories of the flame height (top) and fire-line intensity (bottom) were reported for the same conditions (shrubs, $U_{10}=4$ m/s). We noticed that the sudden increase of flame height observed at the end of the simulation was not associated to a corresponding increase of fire-line intensity (see Fig. 6). Consequently, this sudden modification of fire dynamics cannot be attributed to an acceleration of the propagation of the fires, but can result from an accumulation of unburned pyrolysis products between the two fire fronts. Just before the two fires meet, the mutual interaction between the two fires could promote the formation of pockets of unburned pyrolysis products, which suddenly ignited at the end of the operation. Nevertheless, the conditions contributing to the development of this sudden modification of fire dynamics are not fully understood at this time. Additional studies are necessary to identify, in more detail, all physical phenomena occurring during a counter fire ignition, in order to improve the safety conditions during such a fire-suppression operation. The description of the interactions between the

two fire fronts is quite complex, and they cannot be summarised solely by in-draught flow, generated under some particular circumstances, by the main front. Many other phenomena attest of the interaction between two line fires (a head fire and a back fire) converging towards the same line, for example, the shelter effect induced by the head fire upon the back fire, or the plume interactions. As shown in Fig. 7, representing the temperature field and the velocity vectors at two moments during the propagation of two fire fronts, the dynamics of the back fire were strongly affected by the trajectory of the plume issued from the head fire. The atmospheric flow resulting from this complex

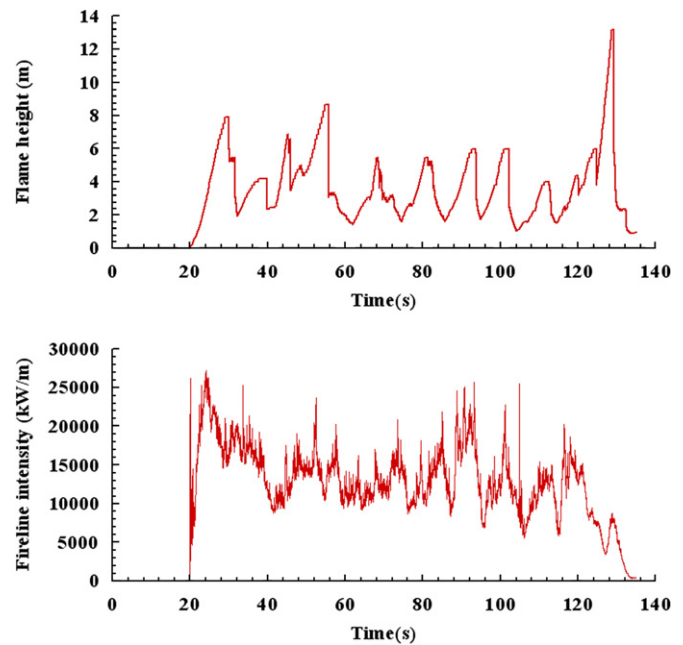


Fig. 6. Time evolution of the flame height (isotherm $T=700$ K) (top) and fire-line intensity (bottom) during suppression fire simulation in Mediterranean shrubland ($U_{10}=4$ m/s).

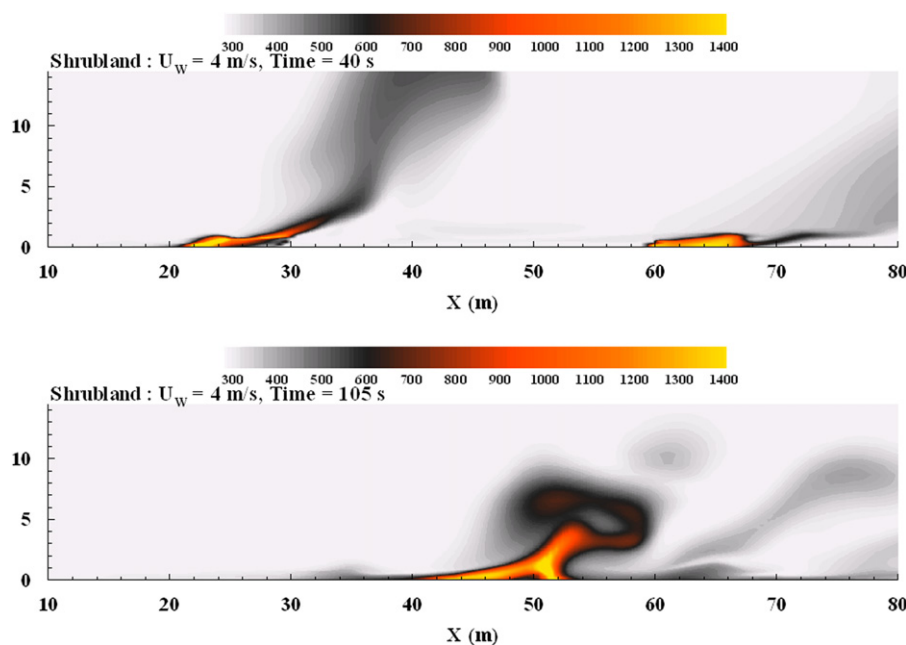


Fig. 5. Temperature field calculated during suppression fire operation carried out in Mediterranean shrubland 40 and 105 s after the simultaneous ignition of the two fires and for wind speed $U_{10}=4$ m/s.

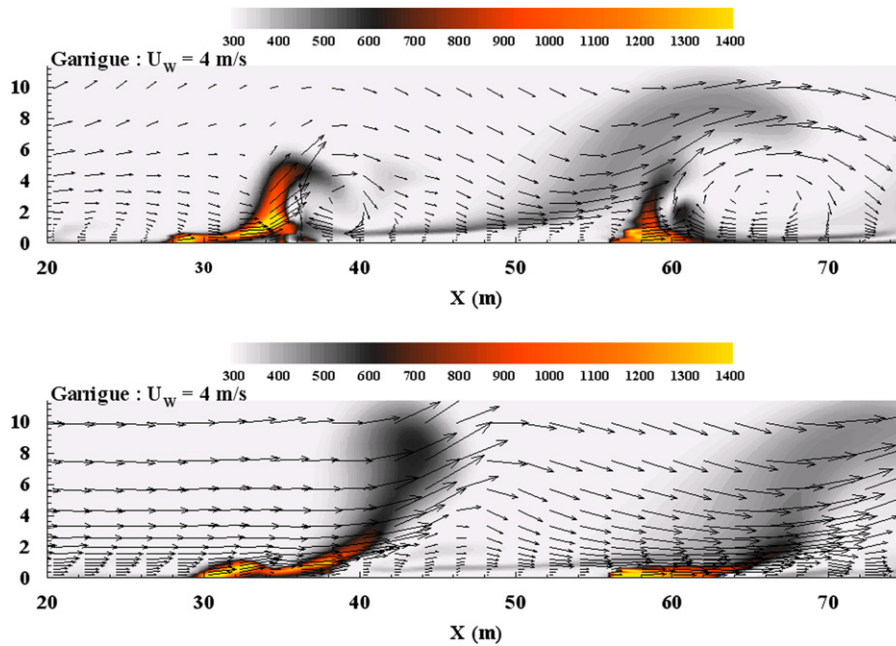


Fig. 7. Temperature field and velocity vectors calculated at two time steps (separated by 4 s) during the simulation of suppression fire operation in Mediterranean shrubland ($U_{10}=4$ m/s), illustrating the strong interaction between the plume and back fire.

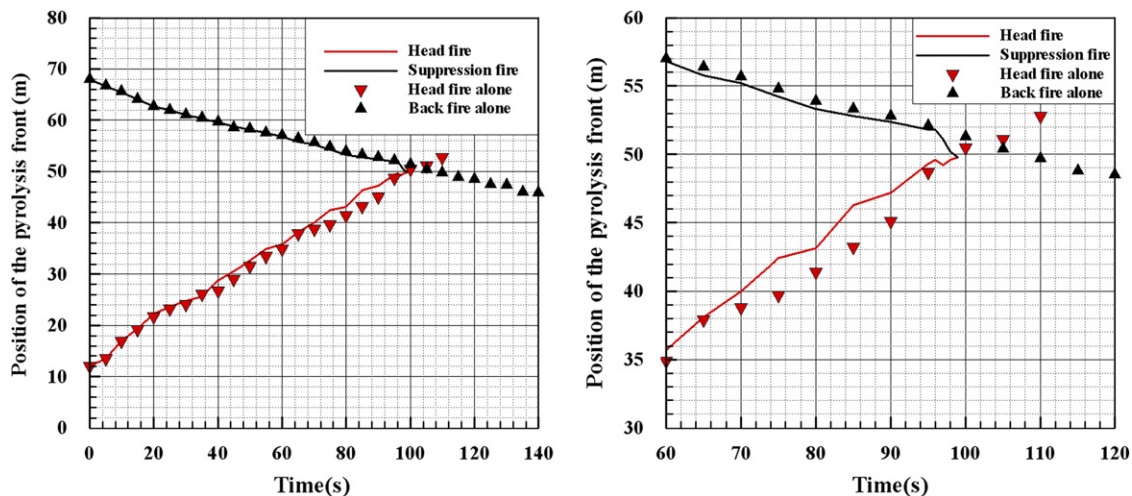


Fig. 8. Time evolution of the pyrolysis fronts (isotherm $T_{Fuel}=500$ K) in Mediterranean shrubland (head fire, suppression fire, head fire alone and back fire alone). A closer view is given on the right.

interaction contributes to promoting (top of Fig. 7), or not (bottom of Fig. 7), the conditions of propagation of the back fire. These two snapshots also highlighted that for moderate wind conditions (here $U_{10}=4$ m/s), the aerology in the vicinity of the fire fronts was strongly affected by the fire itself. In analysing the trajectory of the pyrolysis fronts (isotherm $T=500$ K) inside the fuel layer (Fig. 8), we also noticed that the head fire can also be affected by the presence of the back fire, which can act significantly on the plume trajectory and therefore on the flame dynamics of the main fire front. Consequently, it is not surprising that the dynamics and the interactions between two fire fronts can also be greatly affected by the wind flow conditions. In Fig. 9, we show a snapshot of the temperature field calculated for four wind conditions ($U_{10}=2, 4, 8$ and 12 m/s). From these numerical results, it is evident that the trajectory of the plume from the head fire was strongly deviated horizontally as the wind conditions became more severe. In the same manner, the vertical development of the flame and the plume from the back fire was

drastically reduced, increasing the wind flow conditions. The consequences upon the ROS can be analysed from the curve shown in Fig. 10, representing the evolution of the ROS evaluated from the time evolution of the position of the pyrolysis front inside the fuel layer (the ROS is the slope of this curve). In this curve, the wind velocity was represented as positive for head fires and negative for back fires. Even if the wind conditions significantly modified the general features of the back fire (especially the development of the flame above the vegetation), it seems from this curve (Fig. 10) that the ROS of the back fire was not significantly affected. This result seems to indicate that the heat transfer between the back fire and unburned vegetation occurred mainly near the ground, inside the solid fuel layer, and was less affected by the modifications of the wind flow. We can formulate the same remark concerning the ROS characterising the propagation of the head fire. As the wind velocity was smaller than a threshold value (between 8 and 12 m/s), the modifications of wind conditions weakly affected the propagation of the head fire.

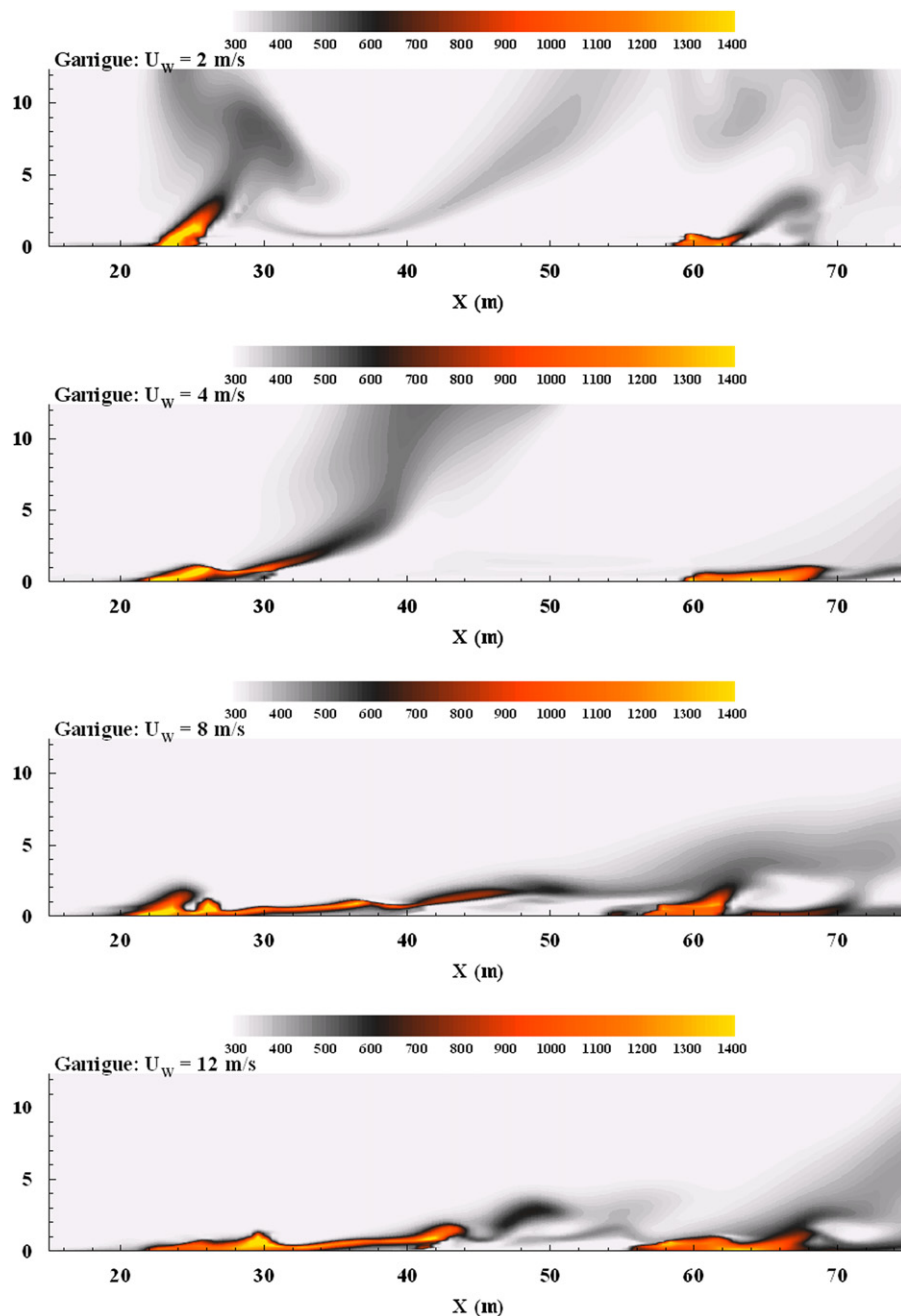


Fig. 9. Temperature field calculated during the suppression fire operation carried out in Mediterranean shrubland for wind speeds $U_{10}=2, 4, 8$ and 12 m/s.

We know that the behaviour of the surface fire is mainly governed by two forces, the inertia due to the wind and the buoyancy. The ratio between these two forces can be approximated from a non-dimensional parameter (the Froude number) as the following:

$$F_r = \frac{U_{10}^2}{gH_f} \quad (3)$$

where g and H_f are the acceleration due to gravity and the average flame height (evaluated in the simulation from the isotherm in the gas phase, $T=700$ K), respectively. For a wind speed within the range 3–15 m/s, the average flame height of a single surface fire decreases from 2.9 to 1.8 m; using this value, the wind speed at which the inertia forces and the buoyancy have the same order of magnitude ($F_r \sim 1$) is nearly equal to 5 m/s. Considering that previously, this change could have a significant effect upon the fire behaviour, the Froude number must be larger than a critical

value (for example, ranged between 2 and 3), the wind speed threshold, separating the two fire regimes (plume dominated/wind driven), could be equal to a value ranging from 6.5 to 7.5 m/s. These results are partially in agreement with previous studies carried out in similar conditions [26,27], confirming that back fires and head fires pushed by a wind flow velocity less than 8 m/s were poorly affected by heat transfer coming from the part of the flame located above the fuel layer. This analysis does not fully explain the results obtained for a head fire in Fig. 10, i.e. the fact that the ROS was not affected by the wind speed until a threshold value equal to 12 m/s was reached. At this stage, it is difficult to conclude between two explanations:

- Due to the value of the fuel moisture content (30%) used, the ROS was more affected by the FMC, and less by the wind speed (until a certain threshold).

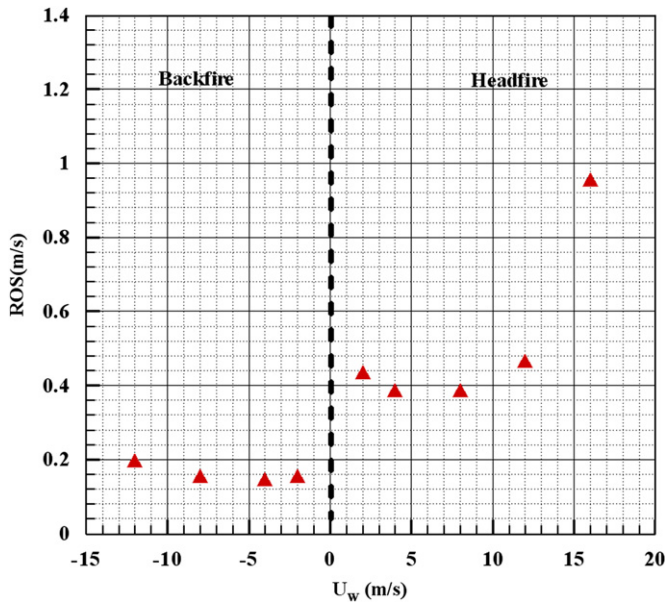


Fig. 10. Rate of spread (ROS) versus 10 m open wind speed velocity U_{10} (U_w in the figure): for a head fire, $U_{10} > 0$, and for a back fire, $U_{10} < 0$.

- A numerical artifact resulting from the 2D hypothesis used in the present simulations.

7. WFDS results for grass fires

Three-dimensional simulations of a fire spreading in a 100 m × 100 m grassland fuel plot were made with WFDS. The fuel properties were the same as those used in the FIRESTAR grassland simulations (see Table 1), and were very similar to the fuel characteristics used in previous WFDS simulations of Australian grass fires. The ignition procedure used here differs from the field procedure [17,18], in which two field workers with drip torches started in the middle of the upwind edge of the fuel plot and walked, in opposite directions, along the fuel plot edge. In the present simulations, the whole width (100 m) of the grassland fuel was ignited at the same time, preventing the propagation of a flank fire. In this way, the fire front maintained a straighter shape that is more consistent with the geometry of the 2D simulations. We know from experimental fires [18,21] and from numerical simulations [17,25] that the development of a flank fire significantly affects the propagation (especially the ROS) of the head fire propagating through grassland. In our case, the absence of flank fires results in head fire spread rates that are higher than those in Australian head fire only grass fire experiments [18,21] and WFDS simulations [17].

When both the head fire and back fire are ignited, we see an overall decrease in the head fire ROS compared to the head fire alone case. This can be seen in Fig. 11, which shows, for a wind speed $U_2 = 2$ m/s, a snapshot of a head fire only simulation (top) and the case with a back fire present (bottom). In the case of a head fire only, the fire line has progressed further in 46 s than in 53 s when a back fire is present. Comparing the two images in Figs. 11 and 13 (the same views from the top) the head fire smoke plume is clearly seen to be affected by entrainment caused by the back fire (i.e. the head fire smoke plume is tilted further downwind when a back fire is present).

The time evolution of the ROS for a head fire and a back fire is plotted in Fig. 12 for both scenarios (again, $U_2 = 2$ m/s). After an initial period of acceleration, the propagation of the head fire,

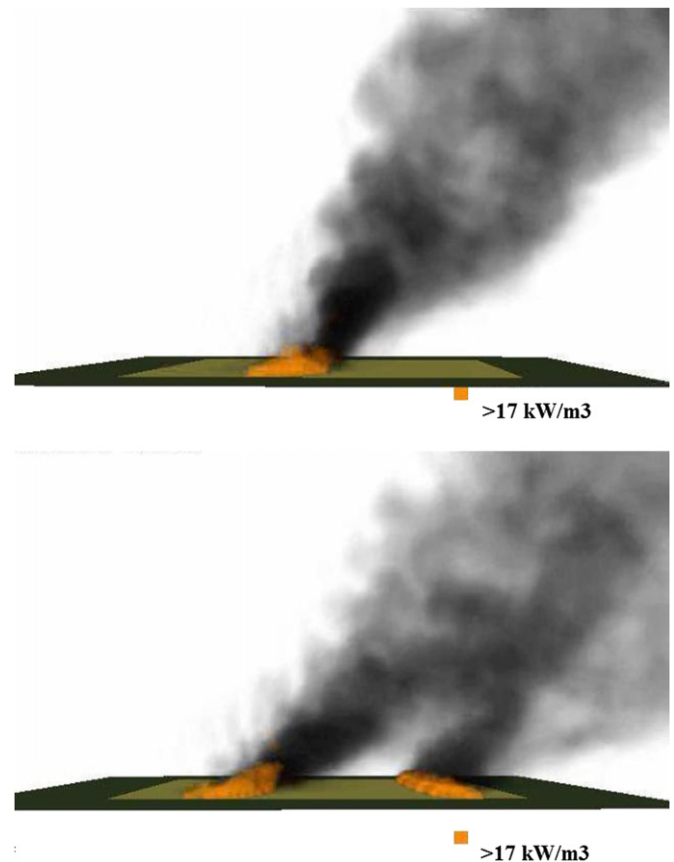


Fig. 11. Numerical simulations (3D) of a single head fire (top) and simultaneous head and back fires (bottom) propagating in grassland for a wind speed velocity $U_2 = 2$ m/s.

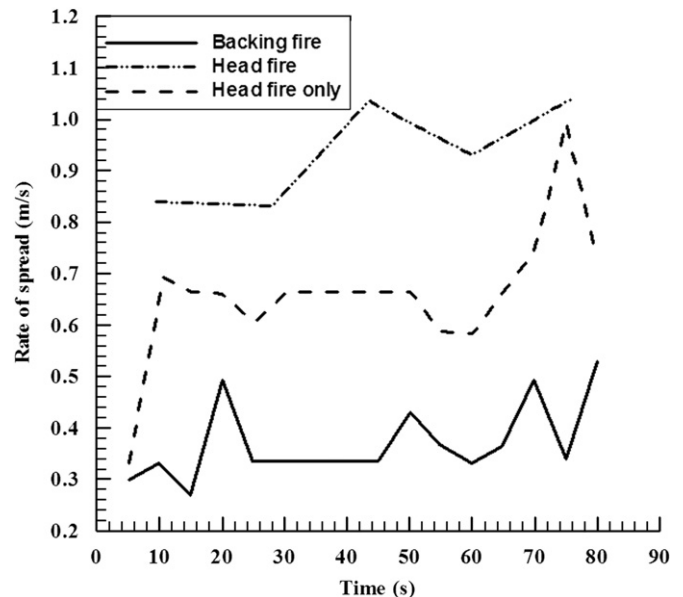


Fig. 12. Rate of spread (ROS) evaluated during 3D simulations of a single head fire and simultaneous head and back fires in grassland.

when a back fire is present, reached a quasi-equilibrium state. After approximately 50 s, the head fire spread rate is more variable. The onset (~50 s) is consistent with head- and back-fire interactions, as seen previously in Fig. 11. The total heat release rate (HRR) time history of the two scenarios is shown in

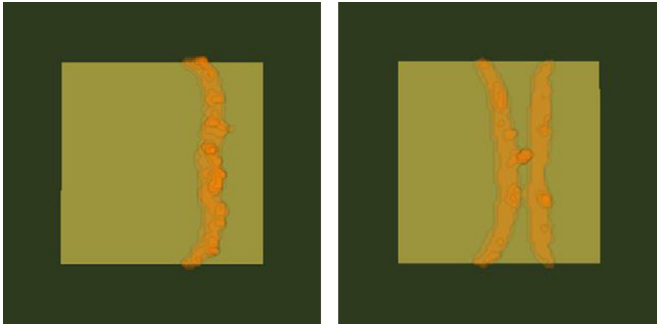


Fig. 13. Top view of the fire fronts 83 s after ignition: single head fire (left), head and back fires (right).

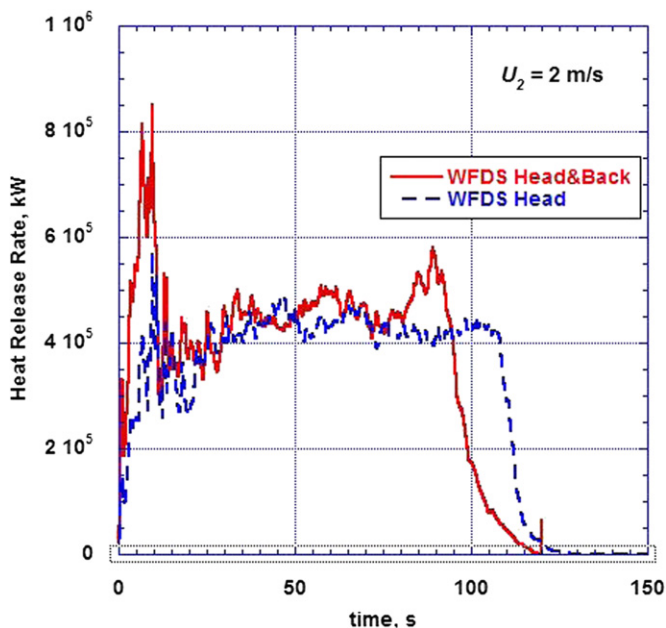


Fig. 14. Time evolution of the heat release rate calculated in 3D using WFDS.

Fig. 14. After an initial period that is influenced by the process of transition from ignition to established fire spread, the two scenarios behave similarly until the head and back fires merge at about 85 s, at which point, a spike in the HRR is evident in the case with a back fire. Conversion of total HRR to approximated fire-line intensities (by dividing the HRR by the width of the fire line) suggests that fire-line intensities varied from 4000 to 4500 kW/m during the steady state period of time for both the head fire only and head- and back-fire simulations. During the merging of the head and back fires, when the spike in the HRR reaches a maximum, the fire-line intensity is 5900 kW/m. This sudden increase of the HRR is in agreement with the increase of the flame height observed with FIRESTAR in Fig. 6. In comparison, for FIRESTAR simulations, we found an average HRR equal to 3809 kW/m for the combustion in the gaseous flame and 2638 kW/m for the smouldering combustion at the surface of the charcoal (this last contribution was not taken into account for the evaluation of HRR in WFDS).

8. Discussion

Comparisons with the average ROS values, before head- and back-fire interactions, obtained using FIRESTAR and WFDS for the

head fires (~ 0.7 m/s WFDS and FIRESTAR) and the back fires (~ 0.3 m/s WFDS and ~ 0.5 m/s FIRESTAR) in the two fire-front simulations, were in a relatively good agreement with each other. Both models also tend to show three clear phases in the interaction of fire fronts: first, the free propagation without significant interaction between the head and back fires, second, a phase during which the two fire fronts interact more significantly, and finally the merging of the two fire fronts into a single fire. In both FIRESTAR and WFDS, the merging of the head and back fires occurred about 83 s after ignition. These results suggest that the two simulation approaches used in this study do produce similar fire behaviour, despite the additional complexity introduced by the third dimension.

There were also differences in the results of the two simulation approaches. In particular, comparisons of the 3D WFDS simulations with and without a back fire suggest that the reduction of the head-fire ROS when a back fire is present may be caused by modifications of the air flow from the sides of the domain. These flow effects cannot be captured with 2D simulations, and may explain why WFDS simulations reported a reduction in head-fire ROS for two fire fronts, while the FIRESTAR simulations did not.

9. Conclusion

Suppression fire operations using a back fire to halt the spread of a head fire were simulated using two fully physical models, in simplified configurations, on a flat terrain, for two types of vegetation layer: Australian grassland and Mediterranean shrubland. The two approaches used in this study both showed clear signs of three distinct phases of interaction between two fire fronts in a suppression fire: first, the free propagation in opposite directions of the head and back fires, second, a phase during which the two fire fronts interact, and finally the merging of the two fire fronts into a single fire. Both simulation approaches also suggested that the merging of the two fire fronts can result in a quick increase in fire-line intensity or in flame height. This sudden event constitutes a potential source of danger for people present during these operations. The results also showed that the behaviour of the back fire and, consequently, its effectiveness, can be greatly affected by the trajectory of the plume of the head fire. The focus of this paper was to determine if physical-based simulations reproduce reasonable and expected head- and back-fire interactions. Further work is required to better understand the complex physical phenomena occurring during a suppression fire operation. Specifically, additional 3D simulation approaches that investigate how the ignition length of the back fire affects this interaction, and 2D and 3D simulations to investigate the effectiveness of suppression fires for more complex fuel beds and different wind speeds. One area that we need to further investigate, concerns scenarios in which the head fire is already fully developed at the time of suppression fire ignition. In addition to further advanced and validated fire behaviour models, there is a real requirement for experimental research involving the interaction of two fire fronts. In particular the change in flow associated with fire-front interactions for different fire-line lengths, greater initial separation of head and back fires, and presence of flanking fires and various ambient wind speeds needs to be investigated further. Such projects would support the evaluation and improvement of simulation methods and the development of empirical rules of thumb that could be useful for fire operation personnel.

References

- [1] C. Chandler, Ph. Cheney, P. Thomas, L. Trabaud, Fire in Forestry, vols. 1 and 2, John Wiley & Sons, 1983.

- [2] J.G. Goldammer, C. De Ronde, *Wildfire Fire Management Handbook for Sub-Saharan Africa*, Global Fire Monitoring Center (GFMC), 2004.
- [3] S.J. Pyne, P.L. Andrew, R.D. Laven, *Introduction to Wildland Fire*, 2nd Edition, John Wiley & Sons, 1996.
- [4] W.M. Pitts, Wind effects on fires, *Prog. Energy Combust. Sci.* 17 (1991) 83–134.
- [5] R. Roxburgh, G. Rein, Study of wildfire in-draft flows for counter fire operations, in: *Proceedings of the Forest Fire 2008, International Conference on Modelling, Monitoring and Management of Forest Fires*, Toledo, Spain, 2008, 10 pp.
- [6] J.L. Coen, S. Mahalingam, J.W. Daily, Infrared imagery of crown-fire dynamics during FROSTFIRE, *J. Appl. Meteor.* 43 (2004) 1241–1259.
- [7] J.L. Coen, Multiple fire interactions, in: Viegas, D.X. (Ed.), *Proceedings of the Fifth International Conference on Forest Fire Research*, 2006.
- [8] D. Morvan, C. Hofman, F. Rego, W. Mell, Numerical simulation of the interaction between two fire fronts in the context of suppression fire operations, in: *Proceedings of the Eighth Symposium on Fire and Forest Meteorology*, 13–15 October 2009, Kalispell, MT, USA, 2009.
- [9] D. Morvan, S. Méradji, O. Bessonov, Interaction between two fire fronts: numerical simulation and physical phenomena, in: *Proceedings of the Sixth International Conference on Forest Fire Research*, Coimbra, Portugal, 15–18 November 2010.
- [10] W. Cui, Q. Qiao, Experimental studies of interactions between back fires and coming surface fires, *For. Stud. China* 4 (1) (2002) 25–28.
- [11] European integrated project Fireparadox FP6-018505: an innovative approach of integrated wildland fire management regulating the wildfire problems by the wise use of fire: solving the fire paradox. <<http://www.fireparadox.org/>>.
- [12] J.A. Vega, C. Jiménez, C. Fernandez, J.L. Dupuy, R.R. Linn, Back fire feasibility in shrubland wildfire fighting in NW Spain, in: *Proceedings of the Sixth International Conference on Forest Fire Research*, 15–18 November 2010, Coimbra, Portugal, 2010.
- [13] J.L. Dupuy, F. Pimont, V. Kononov, R.R. Linn, J.A. Vega, E. Jimenez, A study of backfiring as a wildfire suppression technique using the HIGRAD-FIRETEC model, in: *Proceedings of the Sixth International Conference on Forest Fire Research*, 15–18 November 2010, Coimbra, Portugal.
- [14] A.M. Grishin, *Mathematical Modelling of Forest Fires and New Methods of Fighting Them*, in: F. Albin (Ed.), Tomsk State University, 1996.
- [15] D. Morvan, J.L. Dupuy, Modelling the propagation of a wildfire through a Mediterranean shrub using a multiphase formulation, *Combust. Flame* 138 (2004) 199–200.
- [16] D. Morvan, S. Méradji, G. Accary, Physical modelling of fire spread in grasslands, *Fire Saf. J.* 44 (2009) 50–61.
- [17] D. Morvan, Some physical phenomena contributing to the behaviour of wildfires, in: *Proceedings of the Sixth International Symposium on Turbulence, Heat and Mass Transfer*, Rome, Italy, 14–18 September 2009.
- [18] W. Mell, M.A. Jenkins, J. Gould, Ph. Cheney, A physics-based approach to modelling grassland fires, *Int. J. Wildland Fire* 16 (2007) 1–22.
- [19] N.P. Cheney, J.S. Gould, W.R. Catchpole, The influence of fuel, weather and fire shape variables on fire spread in grasslands, *Int. J. Wildland Fire* 3 (1) (1993) 31–44.
- [20] P.A.M. Fernandes, Fire spread prediction in shrub fuels in Portugal, *For. Ecol. Manage.* 144 (2001) 67–74.
- [21] B.J. Stocks, M.E. Alexander, B.M. Wotton, C.N. Steffner, M.D. Flannigan, S.W. Taylor, N. Lavoie, J.A. Mason, G.R. Hartley, M.E. Maffey, G.N. Dalrymple, T.W. Blake, M.G. Cruz, R.A. Lanoville, Crown fire behaviour in a northern jack pine—black spruce forest, *Can. J. For. Res.* 34 (2004) 1548–1560.
- [22] N.P. Cheney, J.S. Gould, Fire growth in grassland fuels, *Int. J. Wildland Fire* 5 (4) (1995) 237–247.
- [23] D. Morvan, Physical phenomena and length scales governing the behaviour of wildfires: a case for physical modelling, *Fire Technol.* 47 (2011) 437–460.
- [24] P.J. Coelho, Numerical simulation of the interaction between turbulence and radiation in reactive flow, *Prog. Energy Combust. Sci.* 33 (2007) 311–383.
- [25] J. Finnigan, Turbulence in plant canopies, *Annu. Rev. Fluid Mech.* 32 (2000) 519–571.
- [26] R.R. Linn, Ph. Cunningham, Numerical simulations of grass fires using a coupled atmosphere–fire model: basic fire behaviour and dependence on wind speed, *J. Geophys. Res.* 110 (2005) D13107 10,1029.
- [27] D. Morvan, S. Méradji, G. Accary, Wildfire behaviour study in a Mediterranean pine stand using a physically based model, *Combust. Sci. Technol.* 180 (2008) 230–248.